

Energetics and structure of Langmuir monolayers of palmitic acid: a DFT study

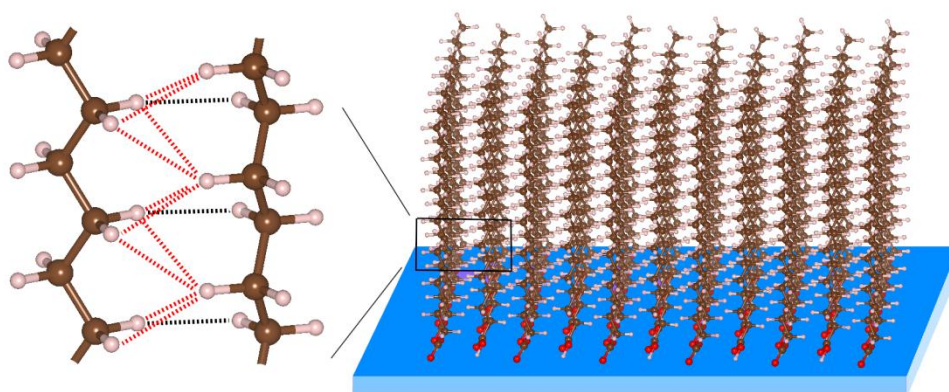
Óscar Toledano and Óscar Gálvez*

Dpto. Física Interdisciplinar, Facultad de Ciencias, Universidad Nacional de Educación a Distancia (UNED), Senda del Rey, 9, 28040 Madrid, Spain

(e-mail: oscar.galvez@ccia.uned.es)

*corresponding author

Key-words: Langmuir monolayer, fatty acid, dihydrogen contact, DFT calculations, van der Waals functional.



Graphical abstract

Supporting Information

1. Monomer of palmitic acid.

Before studying the conformational landscape of the palmitic acid monomer, we analyze the possible conformations of hexanoic acid, for which MP2/TZ calculations can be afforded and compared with the vdW-DF-cx predictions. This conformational analysis has been done for two torsional angles (here named d_{COOH} and d_{OH}) that correspond to the rotation with respect to the alkyl chain of carboxylic and hydroxyl groups, respectively. Figure 1 shows a scheme of the hexanoic acid monomer and the potential energy surface (PES) obtained in MP2/aug-cc-pVTZ calculations for those two torsional angles.

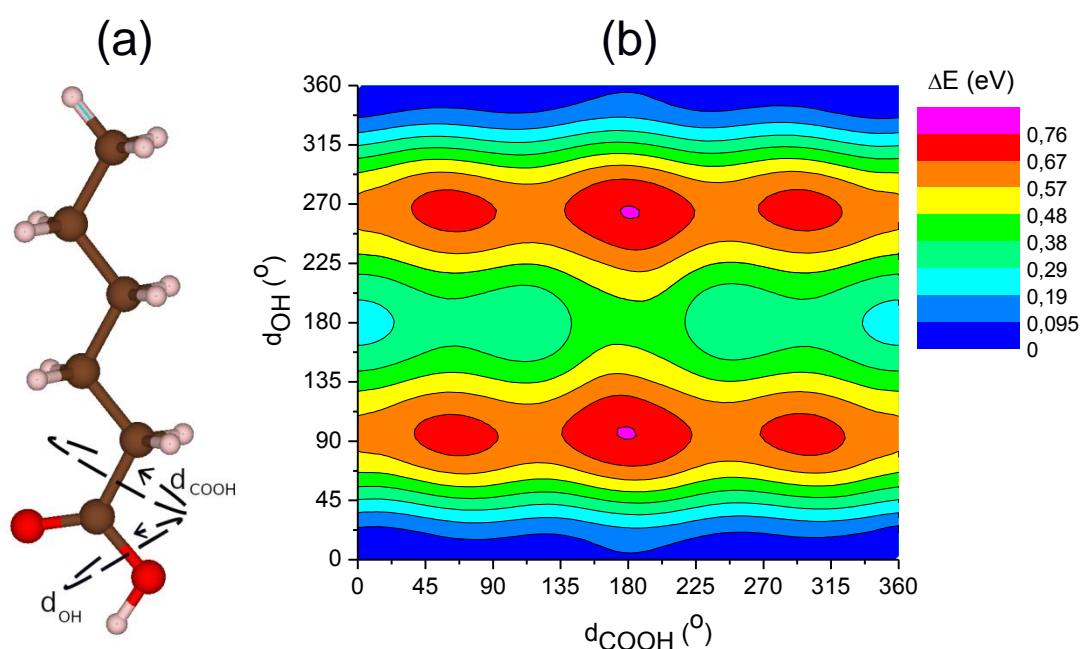


Figure 1. (a) Scheme of hexanoic acid indicating the two torsional used as variables in these calculations. (b) Potential energy surfaces (values in eV obtained in MP2/aug-cc-pVTZ calculations) of the monomer of hexanoic acid represented in terms of the two torsional angles d_{COOH} and d_{OH} . The conformation depicted in (a) corresponds to both d_{COOH} and $d_{\text{OH}} = 0^\circ$.

The energy difference ΔE values (in eV) are calculated with respect to the global minimum that correspond to 0° for both angles (conformation depicted in Fig 1a), a geometry in which carboxylic group lays in the same plane as the carbon chain and O–

H bond points to the water surface. An interesting theoretical study for several fatty acid (from hexanoic to palmitic acid) monomers was performed by Visotsky *et al.* using the PM3 semiempiric method.¹ In that work, a comparable PES obtained upon varying these same torsional angles was computed, presenting a result qualitatively similar to that obtained with the MP2 method. In that work, the global minimum was also found at d_{COOH} and $d_{\text{OH}} = 0^\circ$ while a local minimum was located at $d_{\text{COOH}} = 0^\circ$ and $d_{\text{OH}} = 180^\circ$ that corresponded to a difference of $\Delta H_{298}^0 \approx 0.11$ eV, which is considerably lower than our ΔE_{MP2} value, 0.25 eV. Even though our ΔE values include no enthalpic corrections, as e.g. zero point energy, if one takes into consideration the structural similarities of both minima, these corrections are expected to be very similar for all minima configurations of this system. Therefore, ΔE and ΔH values should be comparable, so that the discrepancies obtained between both studies, must be associated to rather different methodological nature of the quantum calculations involved: semiempiric PM3 vs *ab initio* MP2 method.

Figure 2 shows the potential energy curves obtained through the vdW-DF-cx (red circles) and MP2 (black circles) levels of theory, calculated as a function of only one rotational angle keeping the other angle frozen at 0° . As it is apparent, BH results are in excellent agreement with MP2 results, regarding both curve shape pattern and predicted values.

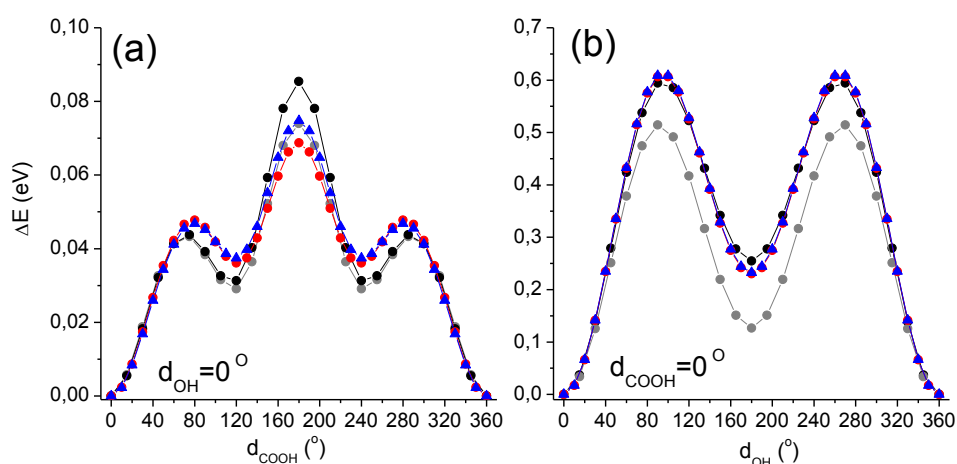


Figure 2. Potential energy curves of hexanoic and palmitic acid monomers as a function of the torsional angles defined in Fig. 1a keeping frozen d_{OH} (a) or d_{COOH} (b) at 0° . Black, gray and red circles correspond to MP2/TZ, MP2/PCM/TZ and vdW-DF-cx/TZ

results for hexanoic acid, respectively. Blue triangles indicate vdW-DF-cx/TZ results for palmitic acid.

It is important to highlight that the rotation of the carboxylic group implies energetic variations of around 0.1 eV, in contrast to the rotation of the hydroxyl group that involves energy differences almost 10 times larger. This result can be explained in terms of the intramolecular interaction between hydroxyl hydrogen and carbonyl oxygen in the global minimum structure (see Fig 1a).

In order to evaluate the influence of the polar sub-phase, we have repeated these calculations in the framework of the solvation model PCM (polarizable continuum model),² one of the most widely used self-consistent reaction field models to simulate the aqueous phase. The results are also included in Figure 2 (gray symbols and lines) and compared with MP2 and vdW-DF-cx simulations. In these calculations, the global minimum (d_{COOH} and $d_{\text{OH}} = 0^\circ$) was also optimized at MP2/PCM/aug-cc-pVTZ method. In the case of the $d_{\text{OH}} = 0^\circ$ curve (Fig. 2a), PCM results are rather similar to those obtained in the gas phase, although more noticeable differences arise when d_{OH} is varied at $d_{\text{COOH}} = 0^\circ$ (Fig. 2b). In this case, the predicted PCM energy difference for the local minimum ($d_{\text{COOH}} = 0^\circ$ and $d_{\text{OH}} = 180^\circ$) is 0.13 eV with respect to the global minimum, to be compared to the 0.25 eV value for the gas phase.

Although it is evident that the aqueous phase must play an essential role in the Langmuir monolayer formation, the use of the PCM approach could not be justified, if one considers that the greater part of amphiphilic molecule in a Langmuir monolayer is exposed to the air phase, contrarily to the treatment provided by the PCM approximation, which considers the whole molecule immersed in a polar solvent. In addition, different experimental studies have shown that the sub-phase changes occurring upon clusterization of aliphatic alcohols produce only a small shift in the temperature boundaries (around 4°C), keeping the structures of the monolayer unit cell nearly unaltered.³ These latter findings are in good agreement with our numerical results, for which PCM predictions show similar tendencies for the potential energy curves as those “gas phase” results obtained with MP2 or vdW-DF-cx methods, finding differences only in the relative ΔE values.

A similar conformational analysis, using only the vdW-DF-cx method, was conducted for palmitic acid monomer, also included in Figure 2. As shown, the results for both molecules are very similar, obtaining a global minimum for $d_{\text{COOH}}=d_{\text{OH}}=0^\circ$ and a local minimum for $d_{\text{COOH}}=0^\circ$ and $d_{\text{OH}}=180^\circ$ at $\Delta E=0.25$ eV in both cases. This result is in good agreement with the report by Visotsky *et al.*,¹ who found an almost indistinguishable ΔH_{298}^0 for hexanoic and palmitic acid (although as the mentioned above, the value was 0.11 eV).

As a general conclusion of this analysis, valid for both gas and aqueous phases, the rotation of the carboxylic group in saturated fatty acid involves overcoming a considerably smaller barrier than the rotation of hydroxyl group (see Fig. 2). Taking into account that thermal energy at 300 K is around 0.025 eV per degree of freedom, the rotation of the carbonyl group could occur inside the Langmuir monolayer at relatively moderate temperatures, whereas the rotation of hydroxyl group should be much hindered, even though PCM results predict a decrease of the torsional barrier with respect to gas phase simulations. This is in agreement with 3D crystalline structures obtained for fatty acids, in which only monomeric structures with $d_{\text{OH}}=0^\circ$ are obtained.⁴ In addition, this result is coincident with the experimental study of Pignat *et al.*^{5,6} for the structure of tilted and un-tilted phases of Langmuir monolayer of fatty acids. In this study, the best fit to the x-ray grazing incidence diffraction data is obtained for carboxyl group geometries with $d_{\text{OH}}=0^\circ$ and $d_{\text{COOH}}=0^\circ$ or 180° .

According to these findings, and in the rest of this report we have only considered monomeric structures with $d_{\text{OH}}=0^\circ$ for the palmitic acid dimers formation allowing the rotation of the COOH group during the optimization.

2. Dimers of palmitic acid. Un-tilted structures.

The simulation of Langmuir monolayers using *ab initio* quantum chemical methods is a challenging study if one considers the long carbon chains of fatty acids, as it is also the case for our study on palmitic acid films. In addition, the large amount of dihydrogen interactions that take place among carbon chains makes a thorough analysis of the conformational landscape of just a dimer a formidable task. However, it is important to highlight that the intermolecular interactions involved in the monolayer formation should be mainly pairwise additive, as the strength of weak dihydrogen contacts dramatically decrease with the distance. We have checked this hypothesis by calculating the interaction energy of a trimer of molecules for two different configurations (see Figure 3 and Table 1).

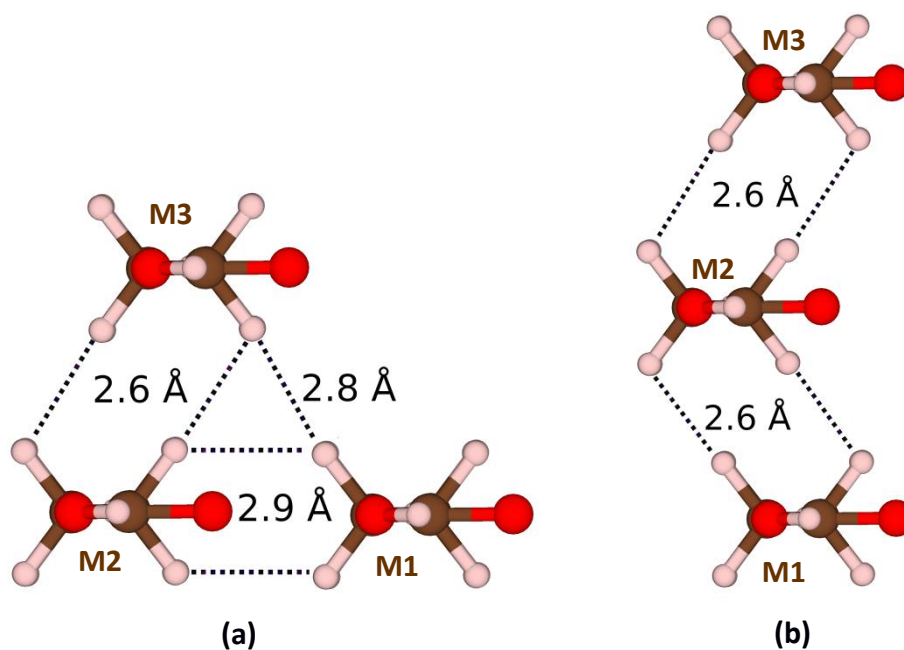


Figure 3. Two different configurations of a trimer of palmitic acid.

Table 1. Dissociation Energies in eV (BSSE correction included) of two different conformers of a trimer of palmitic acid (see Fig. 3).

	ΔE full system	ΔE pairwise interactions
Configuration (a)	-1.30	-1.29
Configuration (b)	-1.11	-1.10

$$^a \Delta E \text{ full system} = E_{\text{trimer}} - E_{\text{monomer1}} - E_{\text{monomer2}} - E_{\text{monomer3}}$$

$$^b \Delta E \text{ pairwise} = \Delta E_{M1-M2} + \Delta E_{M2-M3} + \Delta E_{M1-M3} = E_{\text{dimer-M1-M2}} + E_{\text{dimer-M2-M3}} + E_{\text{dimer-M1-M3}} - 2E_{\text{monomer1}} - 2E_{\text{monomer2}} - 2E_{\text{monomer3}}$$

In these trimers, pairs of monomers M1-M2 and M2-M3 are located at similar intermolecular distances to those belonging to the equilibrium geometries of the corresponding dimers (see Fig. 4). These configurations also are analogous to those obtained for the optimized structures of the monolayers, as discussed below. As can be seen in Table 1, the energies obtained for the full system as a whole and by the addition of dimer interactions are almost identical, confirming that pairwise interaction is the leading mechanism in the clusterization process of long carboxyl acids. This result is also in good agreement with previous studies done by Visotsky *et al.*⁷

We have carried out a thorough conformational analysis of the dimer of palmitic acid. For the dimer construction, we have assumed the equilibrium geometry at the global minimum of the palmitic acid monomer (with torsional angles $d_{\text{OH}} = 0^\circ$ and $d_{\text{COOH}} = 0^\circ$, as shown for hexane monomer in Fig. 1a), relaxing the intermolecular parameters at a tilt angle of 0° in this first case (i.e. variables r , ϕ and θ at $\delta = 90^\circ$ in Fig. 1 from the main text). However, we first verified this assumption by checking the effect of dimer formation on the intramolecular geometrical parameters. Table 2 contains the results of this analysis showing that intramolecular parameters of the palmitic acid molecule were almost unaltered (maximum deviations of only 0.001 Å and 0.04 ° for bond length and angles, respectively, were obtained). For this study we selected conformer “a” (see Fig. 4) for which the shortest dihydrogen contact distances were obtained and the molecular structure might suffer the strongest deformations. This approximation was also assumed in similar computational studies reported by other authors.^{1,8,9}

Table 2. Comparison of intramolecular parameters obtained after dimer formation (structure a in Fig 4), when they were freely relaxed (bond length in Å and bond angles in degrees), with their monomeric values.

	Dimer (mean value)	Monomer (mean value)	Mean deviation	Maximum deviation
C–H _{bonded} ^a	1.128	1.129	0.001	0.001
C–H	1.129	1.129	0.00001	0.0003
C–C–C	113.3	113.3	0.001	0.04
H–C–H	105.9	105.9	0.001	0.03

^aC–H_{bonded} refer to C–H distance for hydrogen participating in dihydrogen contacts.

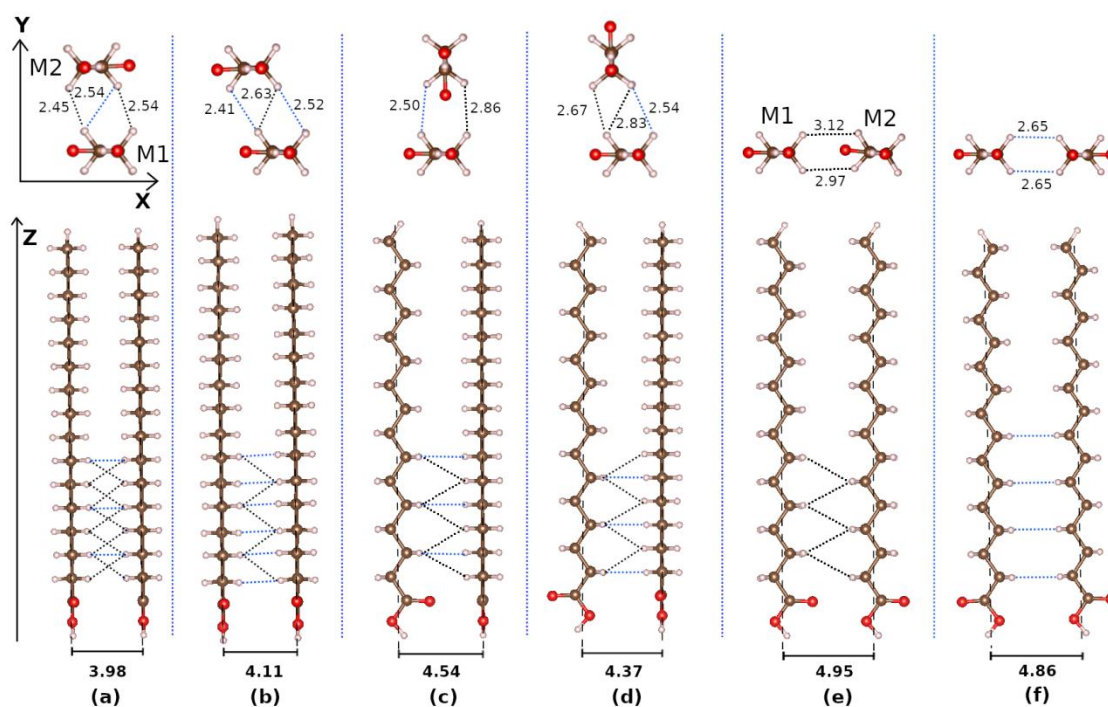


Figure 4. Representation of the six minima found for palmitic acid dimers in un-tilted structures. Upper panel shows a top view, and lower panel a view along the carbon chain. Distances in angstroms. Blue and black dashed lines are *ip* and *oop* dihydrogen interactions respectively.

In order to find all the relevant minima, the complete conformational landscape of the palmitic acid dimer was explored, and the intermolecular parameters r , ϕ and θ (see Fig. 1 from the main text) were varied discretely in step of approx. 0.2-0.3 Å for distance and 15° for angles, always within chemically relevant ranges. As a result of this analysis, six minima were found in which a further relaxation of these intermolecular parameters was allowed (see Figure 4). Finally for some relevant equilibrium configurations, a free rotation of both carboxyl groups was allowed,

obtaining additional minima (results not shown) which differ from those shown in Fig. 4 only in the mutual orientation of carboxyl groups. These minima are only about 0.01 eV from those shown in the figure, consequently they can be considered isoenergetic, and according to the potential energy surface calculated, they could be achieved overtaking potential energy barriers of less than 0.1 eV. These results suggest that, although the structures of these minima have not been discussed, the free rotation of the carboxyl group has been taken into account in the analysis of the monolayer formation, as we will discuss below.

Table 3. Dissociation energies in eV (BSSE correction included) and intermolecular distances (in Å) of the six different conformations of palmitic acid dimer (see Fig. 7).

Configuration	Type 1		Type 2		Type 3	
	a	b	c	d	e	f
Palmitic Acid Dimers						
ΔE	-0.610	-0.535	-0.493	-0.484	-0.368	-0.341
$d_{\text{Chain-Chain}}$	3.98	4.11	4.54	4.37	4.95	4.86
ΔH_{298}^0 ^a			-0.987			
Pentadecane Dimers						
ΔE	-0.524	-0.499	-0.434	-0.421	-0.362	-0.313
$d_{\text{Chain-Chain}}$	3.94	4.15	4.38	4.29	4.78	4.84

^a Ref. 1.

As it is shown in the upper panel of Fig. 4, two axes have been defined for the palmitic acid monomer: the x-axis along the C-C bond in the top-view of the backbone carbon chain and the y-axis perpendicular to it. In addition, z-axis is defined along the long alkyl chain, as it is shown in the lower panel of Fig. 4. Considering these axes, the configurations obtained for the dimers can be classified in three categories:

Configuration type 1: both monomers are aligned parallel to the x-axis but M2 is displaced in the y-axis, as if they were placed one over the other in the xy-plane (see upper panel in Fig. 4). Dihydrogen contacts occur along the plane xy (they also comprise the z axis, as will be discussed below). Considering the orientation of the polar heads, two possible conformations could be obtained: a) the carboxylic groups point to the same direction (polar heads are aligned) or b) carboxylic groups point to opposite directions, obtaining configuration “a” or “b” respectively.

Configuration type 2: it is obtained from a configuration type 1 by rotating M2 monomer 90° and relaxing the structure. Dimers “c” and “d” belong to this type, where monomers lie in a “T”-type conformation (usually named as herringbone, HB) and the intermolecular interactions occur mainly along the y-axis in the xy plane (also along the z-axis as mentioned below). Again two different conformers could be obtained in this type of arrangement depending on the mutual orientation of the polar groups: dimer “c” where the polar head of M2 points to the x-axis of M1, and dimer “d” where both polar heads face outward.

Configuration type 3: in this last case, both molecules are aligned along the x-axis where the dihydrogen contacts are formed. According to the orientation of the polar heads, three different configurations can be obtained. However, when both polar heads point to each other, the resulting conformation is highly unstable due to steric and electrostatic repulsions arising from carbonyl groups. Consequently, the only minima found are dimers “e” y “f” in which both polar heads face to the same direction or outwards, respectively.

It is worthy to highlight that in all the configurations obtained, and perhaps contrarily to certain chemical intuition, monomers are not specifically located in the most symmetric conformation, as e.g. it would occur in a configuration type 1 where M2 would be placed just over M1 (in the same position in the x-axis) in the xy plane. These configurations are not obtained and in the minima M2 is also displaced a specific distance along the x-axis. These “asymmetric” minima configurations could be triggered by different effects, such as, e.g., maximizing the number and strength of dihydrogen contacts formed, achieving the most favorable angular distribution of the C-H...H-C structure,¹⁰ or even by steric factors.

Regarding the arrangement of the atoms involved in the dihydrogen contacts formed, these contacts could be grouped in two main categories: in plane (*ip*) or out of plane (*oop*) interactions. In the first case, the four atoms of the C-H...H-C interaction lie in the same xy plane (see Fig. 5a), and in the second case, a hydrogen atom of a C-H bond is linked to two (or even four, as in dimer “d”) hydrogen atoms belonging to two different alkyl groups located over and under it in the z-axis, so the four atoms of the C-H...H-C interaction are not in the same plane (see Fig. 5b). It is also possible that a

given hydrogen atom could participate in both types of dihydrogen contact (*ip* and *oop*) at the same time (see Fig. 5c), as occur in the configurations type 1 (dimers “a” and “b” in Fig 4). This last circumstance could explain that these dimers are the most stable and present the shortest intermolecular distances.

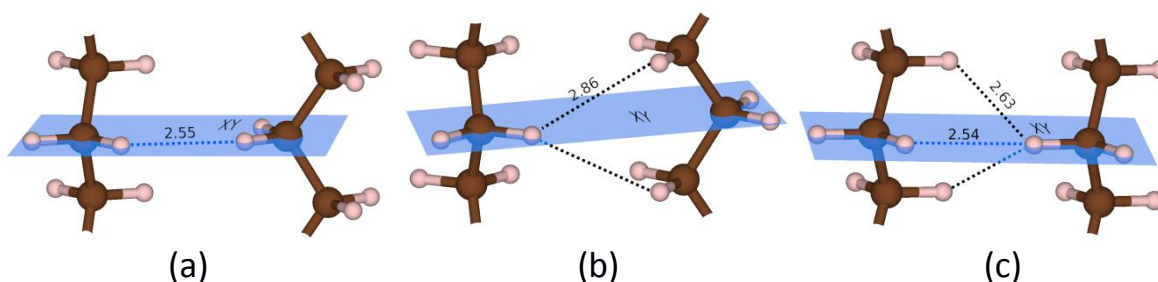


Figure 5. Representation of the in plane, *ip* (a), out of plane, *oop* (b), and in and out of plane (c) types of dihydrogen contacts obtained for the dimers of palmitic acid

Analyzing the distances of both types of dihydrogen interactions separately, i.e., when they do not occur simultaneously for the same hydrogen atom, (situation given in conformers type 2 or 3), *ip* interaction yields shorter distance than *oop* interactions (around 2.5 Å for *ip* and from 2.7 to 2.9 Å for *oop* contacts). However this difference could be compensated by the fact that the *oop* interaction yields twice (or even four) intermolecular contacts for the same hydrogen atom than *ip*, as it has been mentioned before, increasing the number of intermolecular links between monomers.

According to the relative stabilities of the minima found, dimers with configuration type 1 show the highest interaction energies values, being configuration “a” the most stable. In these configurations, all the $-\text{CH}_2$, or terminals $-\text{CH}_3$ groups, participate in the intermolecular interactions (by means of only one C-H bond). As mentioned before, in configurations type 1, both *ip* and *oop* dihydrogen contacts take place simultaneously for the same hydrogen atom, which occurs in 7 C-H bonds per monomer, while the remaining 8 C-H bonds form *oop* (dimer “a”) or *ip* (dimer “b”) interactions. As mentioned above, *oop* contacts, although are in general larger than *ip*, imply the formation of two intermolecular connections, so dimer “a” presents a larger

number of intermolecular interactions than dimer “b” (35 vs 29) which could explain its higher interaction energy (around 0.08 eV).

In the case of dimers in configuration type 2 (“c” and “d”), both *ip* and *oop* interactions occur, although not concurrently for the same hydrogen atom, and similar interaction energies around 0.49 eV are obtained in both conformers. In these dimers, only half of $-CH_2$ groups of one of the monomers (that aligned along the y-axis) participate in dihydrogen contacts, although both hydrogens of these alkyls groups participate in these interactions. In this situation, the electron density and/or valence bond orbitals of the carbon atom, which participates also in a C-H \cdots H-C interaction, should be shared between both hydrogens of the alkyl group (see e.g. the discussion of the nature of C-H \cdots H-C in Ref. 12 in the main text). Consequently these interactions should be weakened with respect to the situation in which only one hydrogen atom of the $-CH_2$ group undergoes the interaction. This condition could explain the larger inter-chain distances predicted for these conformers.

For dimers with configuration type 3, only *oop* interactions takes place in (e) or only *ip* in (f), but not both for the same dimer, and these occur for only half of carbon atoms of each monomer, although the two hydrogens atoms of these $-CH_2$ groups participate in the interaction, as it happens in the previous case. This fact would explain that these conformers present the lowest interactions energies (0.34 - 0.37 eV) and the largest inter-chain distances (around 4.9 Å).

All these results differ in some points from those found by Vysotsky *et al.*¹ on the structure and energetics of palmitic acid clusters. In that work, these authors found ΔH_{298}^0 values range from 0.8 to 1.1 eV for the minima of the dimers, which is approximately double of the values found here. In addition, the configurations of the minima found differ from our predicted geometries, mainly for two reasons: first, a different monomeric structure (with $d_{COOH}=0^\circ$ and $d_{OH}=180^\circ$) was used in the formation of dimers, and second, the polar heads were also allowed to undergo a twist outwards of the backbone plane of the carbon chain. These differences allow for hydrogen bond interactions between carboxylic groups being established, which could justify the higher interactions energies predicted by Vysotsky et al. The presence of other monomeric conformations has been discussed in section 1, concluding that the

rotation of the hydroxyl group implies overtaking a high energetic barrier, so it was not considered in our study. Regarding the twist of the polar head, our exploratory calculations have revealed similar results to that of rotation of the -OH group.

The analysis presented above suggests that the dihydrogen contacts established between alkyl chains, instead of interaction between carboxyl groups of polar heads, determine the global configuration of amphiphilic molecules when the dimers are formed. In order to corroborate this hypothesis we have calculated the most stable configurations of the dimer of pentadecane chain ($C_{15}H_{32}$). Six similar minima structures have been obtained (Figure 5), and the interaction energy and intermolecular distances are included in Table 3. As shown in the figure, in general, the structures are similar to those found for palmitic acid dimers, although, due to both steric factors and interactions between polar heads, some differences are found even though the arrangement of the molecules remains comparable. In addition, the inter-chain distances and the number of *ip* or *oop* dihydrogen contacts in each type of dimer are analogous. Regarding the interaction energy, dimers of palmitic acid are slightly more stable than pentadecane dimers, the larger differences (less than 0.09 eV) arising for the most stable dimers. It must be highlighted that the different configurations obtained show an associated relative energy ordering among them, similar to the one of palmitic acid. This result again suggest that the polar heads instead of leading the intermolecular interactions between fatty acid monomers, strengthen the dihydrogen contact formed among their alkyl chains, especially those with shorter distances. However, further research is needed to completely clarify this effect.

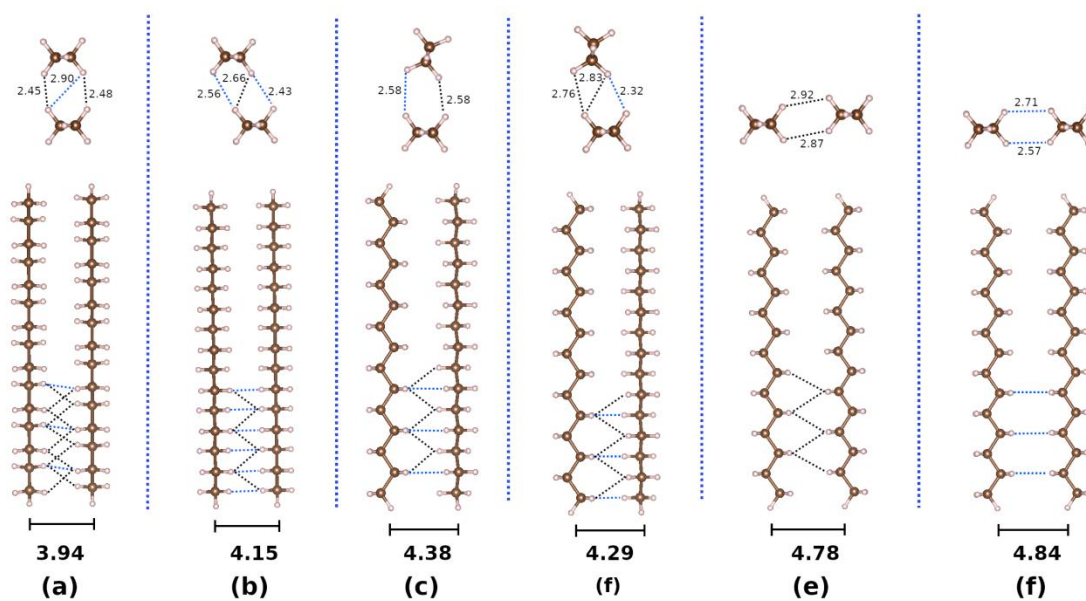


Figure 5. Representation of the six minima found for pentadecane dimer in un-tilted structures. Upper panel shows a view from above, and lower panel a view along the carbon chain. Distances in angstroms. Blue and black dashed lines are *ip* and *oop* dihydrogen interactions respectively.

References

1. Y.B. Vysotsky, D.V. Muratov, F.L. Boldyreva, V.B. Fainerman, D. Vollhardt, and R. Miller, *J. Phys. Chem. B* 2006, **110**, 4717-4730.
2. J. Tomasi, B. Mennucci and R. Cammi, *Chem. Rev.*, 2005, **105**, 2999–3094.
3. H. Kraack, B.M. Ocko, P.S. Pershan, E. Sloutskin, L. Tamam, and M. Deutsch, *Langmuir* 2004, **20**, 5386-5395.
4. E. Moreno-Calvo, G. Gbabode, R. Cordobilla, T. Calvet, M. A. Cuevas-Diarte, P. Negrier, D. Mondieig, *Chemistry-A European Journal*, 2009, **15**, 13141-13149.
5. J. Pignat, J. Daillant, L. Leiserowitz, and F. Perrot, *J. Phys. Chem. B*, 2006, **110**, 22178-22184.
6. J. Pignat, J. Daillant, S. Cantin, F. Perrot, O. Konovalov., *Thin Solid Films*, 2007, **515**, 5691–5695.
7. Y. B. Vysotsky, E. S. Kartashynska, E. A. Belyaeva, V. B. Fainerman, D. Vollhardt and R. Miller, *PCCP*, 2015, **17**, 28901-28920.
8. L. Ferrighi, Y. X. Pan, H. Grönbeck and B. Hammer, *The Journal of Physical Chemistry C*, 2012, **116**, 7374–7379.
9. S. Tsuzuki, K. Honda, T. Uchimarui and M. Mikami, *J. Phys. Chem. A*, 2004, **108**, 10311–10316.
10. D. Danovich, S. Shaik, F. Neese, J. Echeverría, G. Aullón and S. Alvarez, *J. Chem. Theory Comput.*, 2013, **9**, 1977–1991.